ANALYSIS OF THE OECD MAIN STEAM LINE BREAK BENCHMARK PROBLEM USING THE REFINED CORE THERMAL-HYDRAULIC NODALIZATION FEATURE OF THE MARS/MASTER CODE

THERMAL HYDRAULICS

KEYWORDS: *MARS/MASTER code, coupled spatial kinetics and thermal hydraulics, OECD MSLB benchmark*

HAN GYU JOO,* JAE-JUN JEONG, BYUNG-OH CHO, WON JAE LEE, and SUNG QUUN ZEE *Korea Atomic Energy Research Institute*
150 Deokjin Dong, Yuseong, Daejeon, 305-353, Korea

Received November 2, 2001
Accepted for Publication November 11, 2002

The refined core thermal-hydraulics (T-H) nodalization feature of the MARS/MASTER code is used to generate a high-fidelity solution to the OECD main steam line break benchmark problem and to investigate the effects of core T-H nodalization. The MARS/MASTER coupling scheme is introduced first that enables efficient refined node core T-H calculations via the COBRA-III module. The base solution is generated using a fine T-H nodalization consisting of fuel assembly–sized radial nodes. Sensitivity studies are performed on core T-H nodalization to examine the impacts on core reactivity, power distribution, and transient behavior. The results indicate that the error in the peak local power can be very large (up to 25%) with a coarse T-H nodalization because of the inability to incorporate detailed thermal feedback. A demonstrative departure from nucleate boiling (DNB) calculation shows no occurrence of DNB in this problem.

I. INTRODUCTION

Numerous coupled system thermal-hydraulics (T-H) and three-dimensional (3-D) kinetics codes have been developed in recent years, and their performance has been examined for the Organization for Economic Cooperation and Development (OECD) main steam line break (MSLB) problem.[1] The MARS/MASTER code[2] is one of such codes developed at Korea Atomic Energy Research Institute by combining the MARS multidimensional system T-H code[3] and the MASTER neutronics code.[4] The MARS/MASTER code has several unique features that are distinguished from others. One of them is the feature of 3-D flow representation for the vessel, and the other is the ability of employing assembly or its quarter-sized radial T-H nodes for the core T-H calculation. While the former feature provides better flow mixing and cross-flow prediction capability than the quasi-3-D flow models, the latter allows more accurate calculation of the local power than coarse T-H node models through the incorporation of detailed feedback effects. In addition, the MARS/MASTER code can generate departure from nucleate boiling (DNB) ratios (DNBRs) during the coupled transient simulation for each hot pin defined in every radial node.

There are two primary concerns in the analysis of the steam line break accident: return-to-power and DNB. The coupled codes are required to address these concerns in the best-estimate manner. Since return-to-power is a globally occurring phenomenon, sufficiently accurate prediction of the core power level would be possible if the transient inlet coolant condition and the core reactivity are properly determined by the coupled code. DNB is, however, a local phenomenon, and thus the accuracy of the calculated DNBR depends on the accuracy of the power distribution as well as the global core power level. In this regard, the refined core T-H nodalization feature of the MARS/MASTER code is valuable because incorporation of the detailed thermal feedback is crucial in producing accurate power distributions. In the work here, this feature is utilized first to generate a high-fidelity solution to the OECD MSLB benchmark problem and then to investigate the effects of core T-H

*E-mail: joohan@kaeri.re.kr

nodalization on the global core power, local DNBR, and other parameters of interest.

In the MARS/MASTER code, two coupling schemes are available, and they are distinguished by the way the MARS module is coupled to the MASTER modules as shown in Fig. 1. In the single coupling scheme, MARS is connected only to the power calculation module of MASTER, whereas in the double coupling scheme, MARS is connected additionally to the core T-H module of MASTER. The double coupling scheme provides the refined core T-H nodalization feature since the internal T-H module of MASTER, COBRA III-C/P (Ref. 5), is well suited for fine mesh calculations. In Sec. II, the two coupling schemes and the coupled transient time step control logic are described in more detail. For a coupled calculation, MARS/MASTER needs three types of input models. The first one is the MARS T-H model, while the second and third ones are the MASTER neutronic model and the COBRA core T-H model, respectively. The MARS/MASTER model developed to produce a highly accurate solution to the OECD MSLB problem is introduced in Sec. III along with the results. It is then followed by Sec. IV, which describes the sensitivity studies performed on core T-H nodalization. Four models involving different radial and axial core T-H nodalization schemes are examined to investigate the effect of node sizes on global and local characteristic parameters during the transient as well as at the steady-state conditions. A demonstrative DNB calculation is presented in Sec. V, which is performed to examine the possibility of the occurrence of DNB in this MSLB problem. Section VI concludes the paper.

II. MARS/MASTER COUPLING SCHEMES

When MARS/MASTER was first developed, only the single coupling option was available so that only coarse node core T-H calculations were possible. Previous MARS/MASTER MSLB exercise III solution to the OECD/MSLB problem[2] was obtained using a coarse T-H nodalization. The double coupling option that enables refined node core T-H calculations was recently implemented.[6] Since the features of the MARS/MASTER code have been introduced by earlier publications,[2,7] this section describes only the particular characteristics of the MARS/MASTER code relevant to the double coupling.

The backbones of the MARS code are the RELAP5/MOD3 and COBRA-TF codes (Refs. 8 and 9, respectively), which provide the bases of the one-dimensional (1-D) and 3-D modules of MARS, respectively. The 3-D module is used for realistic representations of the T-H field within the reactor vessel, whereas the 1-D module is used for the rest of the system. The coupling of the 1-D and 3-D hydrodynamic models is achieved by solving an implicitly coupled system pressure matrix equation. This solution scheme imposes practical limitations on the core node sizes. If fine nodes are used for the core, the number of nodes increases significantly, resulting in a large pressure matrix that will require an excessive solution time. In addition, the smaller time step sizes resulting from the reduced Courant limit further increase the computing time. Thus, sufficiently large nodes are used in the MARS calculation.

As far as thermal feedback effects are concerned in the coupled calculation, however, the use of coarse T-H nodes causes a nontrivial impact on the power distribution. Since several neutronic nodes are represented by one T-H node, the values of a T-H feedback variable of those neutronic nodes are the same. Under this circumstance, the feedback effect at a higher-power neutronic node is underestimated. The underestimation of the feedback effect causes a higher power than the case with detailed feedback. The opposite effect occurs at lower-power nodes. Consequently, the power distribution

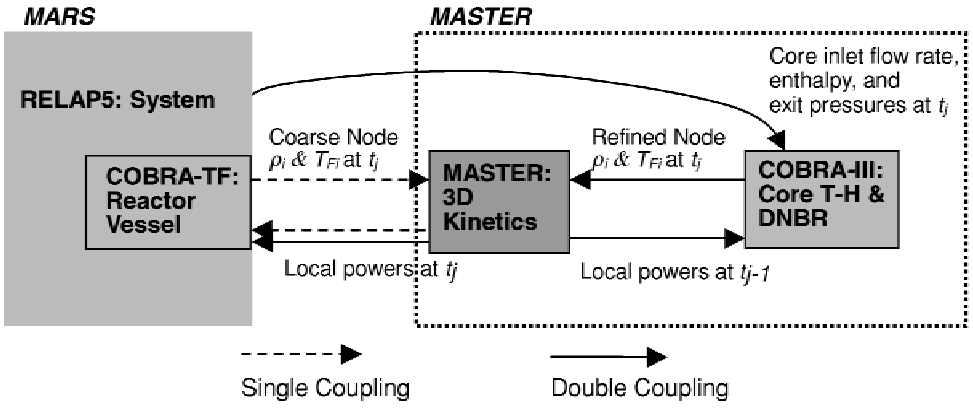

Fig. 1. Data flow in the MARS/MASTER coupling schemes.

obtained with a coarse T-H nodalization is more spatially fluctuating, and the peaking factor becomes higher. This is conservative but needs to be avoided to restore any available margin. This need provided one motivation for the activation of the COBRA-III T-H module of MASTER for additional separate core T-H calculation. The COBRA-III module employs the same radial node structure as the neutronics, and thus, T-H calculations with one node or four nodes per assembly can be performed. The computational requirement for this fine node T-H calculation with COBRA-III is much smaller than with MARS since COBRA-III is based on a much simpler formulation, homogeneous equilibrium model and employs an efficient iterative 3-D solution method. In addition, various DNBR calculation schemes were already available in the COBRA-III module. This provided the other motivation for the use of the COBRA-III module in the coupled calculation to predict the transient DNBR behavior.

Similar coupling schemes to the two MARS/MASTER coupling schemes were reported for the RELAP/PANBOX (R/P/C) coupled code.[10] The internal integration of the R/P/C code corresponds to the single coupling of the MARS/MASTER code, whereas the external integration corresponds to the double coupling. The primary difference between the two codes lies in the flow representation scheme for the vessel regions in the system-vessel coupled flow calculation. MARS employs the COBRA-TF module for a full 3-D flow representation within the vessel. In Secs. II.B and II.C, the two coupling schemes of MARS/MASTER are described in more detail.

In the coupled calculations involving various kinds of physical phenomena yielding different characteristic time constants, it is important to establish an efficient coupled calculation control logic in order to avoid unnecessary calculations. MARS/MASTER has a simple control logic to save much of the spatial kinetics computing time during the coupled calculation. This logic is explained in Sec. II.C.

II.A. Single Coupling for Coarse Core T-H Nodalization

In the single coupling mode, the core T-H calculation is performed solely by MARS. The 3-D component of a MARS model, which is responsible for the core as well as the rest of the vessel regions, represents the core with several hydraulic volumes and heat structures. These T-H nodes are chosen to be generally large enough to contain tens of fuel assembly (FA)–sized neutronic nodes for computing efficiency. For coupled calculations, therefore, a mapping between the neutronic nodes and T-H nodes must be established. The mapping is specified in MARS/MASTER by a user input that provides both radial and axial mapping information.

Normally, a neutronic node belongs entirely to a T-H node since the T-H nodes are larger. However, there could be some neutronic nodes that belong to multiple T-H nodes. Examples are the neutronic nodes located on the symmetric axis or a hot pin channel belonging to an assembly channel. In order to handle these possibilities, the MARS/MASTER mapping input is constructed such that all the T-H nodes belonging to a neutronic node are specified with their respective node number and volume fraction within the neutronic node. The mapping information is given separately for the radial and axial directions, and thus, different radial mapping on different axial planes is not possible. On the other hand, the same mapping specification is used for both a hydrodynamic volume and its corresponding heat structure. The possibility of using multiple heat structures in one hydrodynamic volume is thus not allowed in the MARS/MASTER modeling.

When transferring T-H field information from MARS to MASTER, a weighted average of the T-H field variables of the T-H nodes belonging to a neutronic node is used. On the contrary, a weighted sum of the neutronic nodal powers of all the neutronic nodes belonging to a T-H node is transferred from MASTER to MARS. Since there are several neutronic nodes belonging to the same T-H nodes, many nodes can have the same value for a T-H field variable in the single coupling scheme.

T-H codes generally calculate node properties such as fluid temperature and density at the exit point of a node, not at the center point. This is true with the MARS module as well. Since the node average values are required for the T-H feedback calculations in the MASTER module, node average values of coolant temperature and density are obtained for each T-H node by taking the average of two node exit values before performing T-H to neutronics mapping.

II.B. Double Coupling for Refined Core T-H Nodalization

The COBRA-III module in MASTER was originated from COBRA III-C/MIT (Ref. 5). In the COBRA module, the continuity, energy, axial momentum, and transverse momentum equations governing the thermal-hydraulic field are solved as a boundary-value problem employing the homogeneous equilibrium model. The boundary conditions to be specified are the inlet enthalpy (or temperature), inlet axial flow, and exit pressure. Normally, these boundary conditions are specified as predetermined time-dependent forcing functions given in a tabular form. If these forcing functions are specified by a system code during the transient calculation, coupled calculations can be possible.

The coupling scheme to incorporate the COBRA-III module for refined core T-H nodalization was established such that MARS provides COBRA-III with the forcing functions at every time step. In this scheme, which

is represented by the solid lines in Fig. 1, the T-H calculation for the core regions is performed twice at each time step. The first calculation is performed by MARS with a coarse nodalization, and thus, the effect of the system T-H behavior can be propagated properly to the core T-H condition. The second calculation is by COBRA-III with a refined nodalization (radially, assembly, or its quarter-sized nodes). At the inlet, the boundary conditions are specified in the coarse node base, but the distributions within the core are obtained in the fine node base. The sum of the mass flow rates over the fine nodes belonging to a coarse node is made to be the same as the coarse mesh value that is used for the COBRA-TF calculation. The same thing is true for the inlet enthalpy and the volumetric power distribution. This ensures consistency between the COBRA-III and COBRA-TF energy transfer calculations. The temperature and density information determined by the COBRA-III module for the fine mesh is passed to the MASTER's neutronics module, and the neutronics module calculates the new power distribution based on the nodal cross sections determined using the fine T-H information. MARS uses the new power distribution at the next time step. As shown in Fig. 1, MARS is coupled to the T-H module as well as the neutronics module of MASTER, which signifies the *double* coupling.

Thermal-hydraulically, the COBRA-III solution does not have any impact on the MARS solution because there are no connections between the COBRA-III output variables and MARS input variables. However, the COBRA-III solution has indirect effects on the MARS solution through the power distribution, which is affected by the COBRA-III output variables. Therefore, the results of the MARS/MASTER coupled calculations with and without the COBRA-III module are slightly different.

II.C. Coupled Calculation Control Logic

The simplest method for controlling the T-H and neutronics coupled calculation is the plain explicit method in which one pair of T-H and neutronics calculations is performed at each time step. Normally, the T-H calculation leads the neutronics in that the T-H field at the end of the time step is determined first and subsequently the power distribution is updated. In the plain explicit method, the *common* time step size should be the smallest of the two time steps determined separately by the two solution modules. In general, the coupled calculation is applied to neutronically slow transients in which no rapid power excursion occurs. In such cases, the neutronic time step size can be much larger than the required T-H time step sizes often limited by the Courant limit or stability considerations.

If the neutronics calculation is performed with much smaller time step sizes than necessary, it takes a much longer time for the coupled calculation without gaining accuracy. For efficient calculation, therefore, it would be wise to skip some of the neutronics calculations by advancing only the T-H calculation. In this regard, a cumulative explicit method was implemented in MARS/MASTER, in which advancing the MARS T-H calculation continues until the accumulated time step size reaches the desired MASTER neutronic time step size. The COBRA-III calculation is performed also with the accumulated time step size. This coupled calculation control scheme was proved very effective in reducing the computing time although it takes somewhat longer to converge the neutronics solution at each time step with longer time step sizes.

III. MSLB ANALYSIS MODELS AND BASE RESULTS

For the MARS/MASTER coupled calculation, the input models for the MARS and MASTER codes need to be prepared separately. The MARS model consists of two parts: the 1-D system input and the 3-D vessel input; the MASTER model consists of three parts: the base neutronics input, the COBRA-III input, and the MARS/MASTER mapping input. In the following, the MARS/MASTER input data generated for the OECD MSLB benchmark problem are described. The base MARS/MASTER results were obtained using this model, which involved a refined core T-H nodalization. Various aspects of the base results are examined later in this section.

III.A. MARS and MASTER MSLB Models

The Three Mile Island Unit 1 (TMI-1) system nodalization generated for MARS MSLB analyses is given in Fig. 2. The MARS 1-D system model consists of 157 volumes that constitute the reactor coolant system (RCS), pipes, pumps, pressurizer, steam lines, steam generators (SGs), and valves. While the system modeling is 1-D, a 3-D flow model is applied to the reactor vessel as shown in Fig. 3. The MARS vessel model consists of 3 axial sections (divided into 14 axial levels), 4 or 5 radial shells, and 6 azimuthal sectors. This nodalization results in 59 channels, 95 gaps, and 374 volumes. The vessel model is linked to the system model through the hot and cold legs that are connected to vessel channels 44, 47, 49, 51, 52, and 54 at axial level 8. The flow mixing in the lower and upper plena, which is given in the problem specification,[1] was satisfied by properly selecting the form loss coefficients of the relevant channels and gaps.[2]

The active core is modeled using 18 flow channels (channels 25 through 42) and 6 axial meshes in Sec. II. Each of the channels contains a heat structure to model the average fuel rod in the channel. The average rod represents the fuel rods contained in about ten fuel assemblies.

The neutronic nodalization in the MASTER model consists of 241 radial nodes (177 fuel nodes and 64 reflector nodes) and 28 axial nodes. For coupled calculation

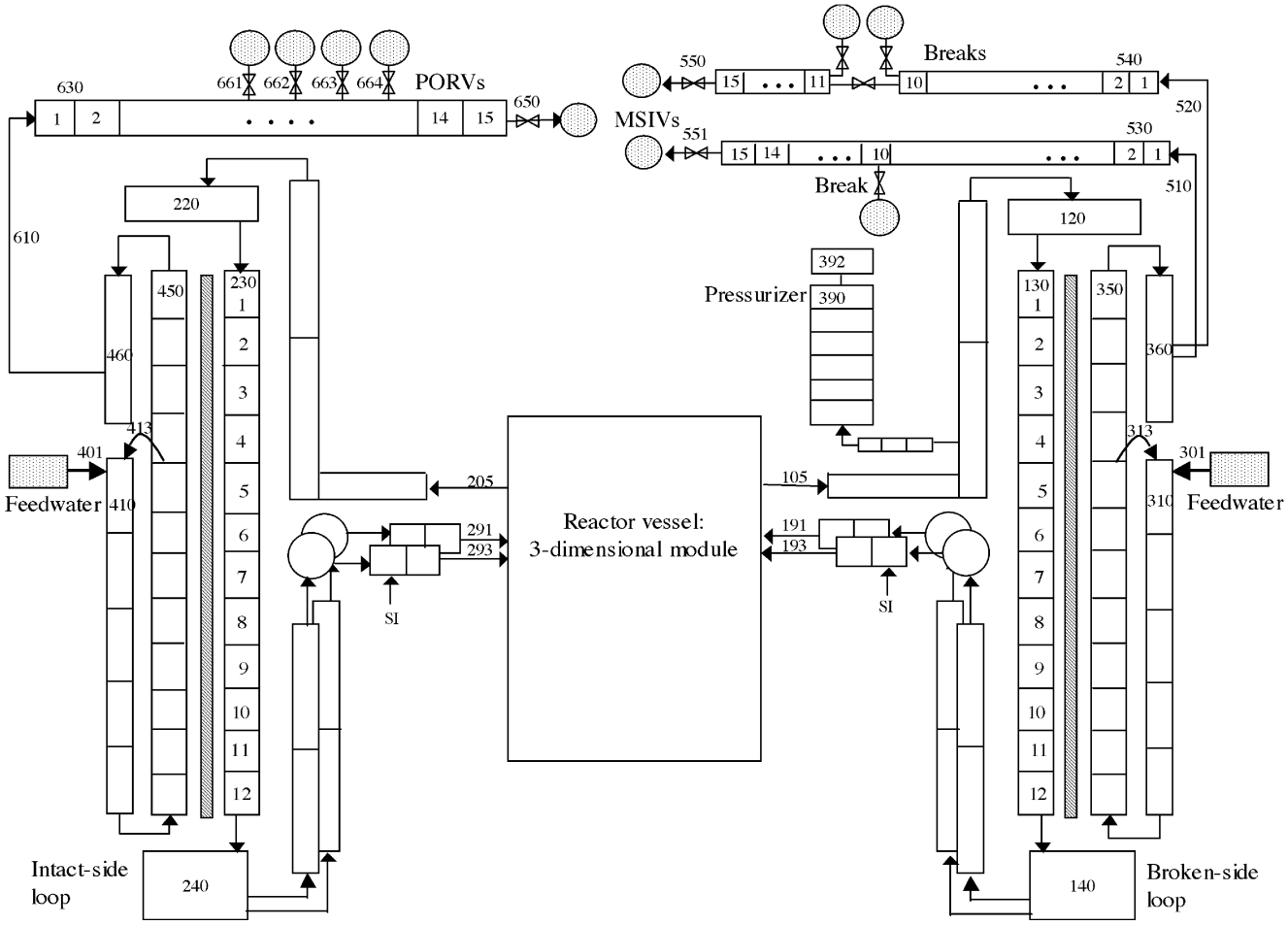

Fig. 2. TMI-1 system nodalization for MSLB analysis.

with MARS, the neutronic nodes are mapped into the T-H nodes both radially and axially. The radial mapping scheme employs the neutronic node to channel correspondence established for exercise II of the benchmark (Fig. 3.2.3 of Ref. 1; refer to Fig. 13 as well). According to this correspondence, the T-H nodes belonging to the innermost region are assigned to 7.5 neutronic nodes, whereas the T-H nodes in the middle shell and those in the outer shell are assigned to 10 and 12 neutronic nodes, respectively. Axially, 4 to 6 axial neutronic nodes are assigned to a T/H node. On the other hand, the COBRA-III model consists of 177 channels and 24 axial levels. The channels are connected through 354 gaps so that cross flow between channels can be modeled. Among the two cross-section sets specified for this benchmark, the return-to-power set in which the control rod cross sections are reduced are used in this analysis.

III.B. Steady-State Results

The base case of the MARS/MASTER MLSB analyses was performed with the double coupling option to activate the COBRA-III refined core T-H calculation. The primary steady-state output parameters are listed in Table I. As shown in Table I, most of the MARS-calculated system parameters conform to the design specification values very well. One exception is noted for the SG inventory. Since the overcooling of the primary coolant continues until the SG empties, it would be important to get the SG inventory right. However, because there is an additional mass of water (~16 000 kg) filling the feed-line pipe between the SG inlet nozzle and the feedwater isolation value, this difference of ~1000 kg is not significant. On the other hand, the k_{eff} of 1.00361 is quite low compared to the single coupling case employing the coarse core T-H nodalization (e.g., 1.00580 in Ref. 2). The reasons for the lowered reactivity with the refined core T-H nodalization will be elaborated in Sec. IV.A.

One of the distinguished features of the MARS code is the 3-D flow representation for the vessel. In order to demonstrate this feature, the flow distributions obtained at the inlet and outlet of the active core are listed in Table II. Table II shows that flow entering the inner region

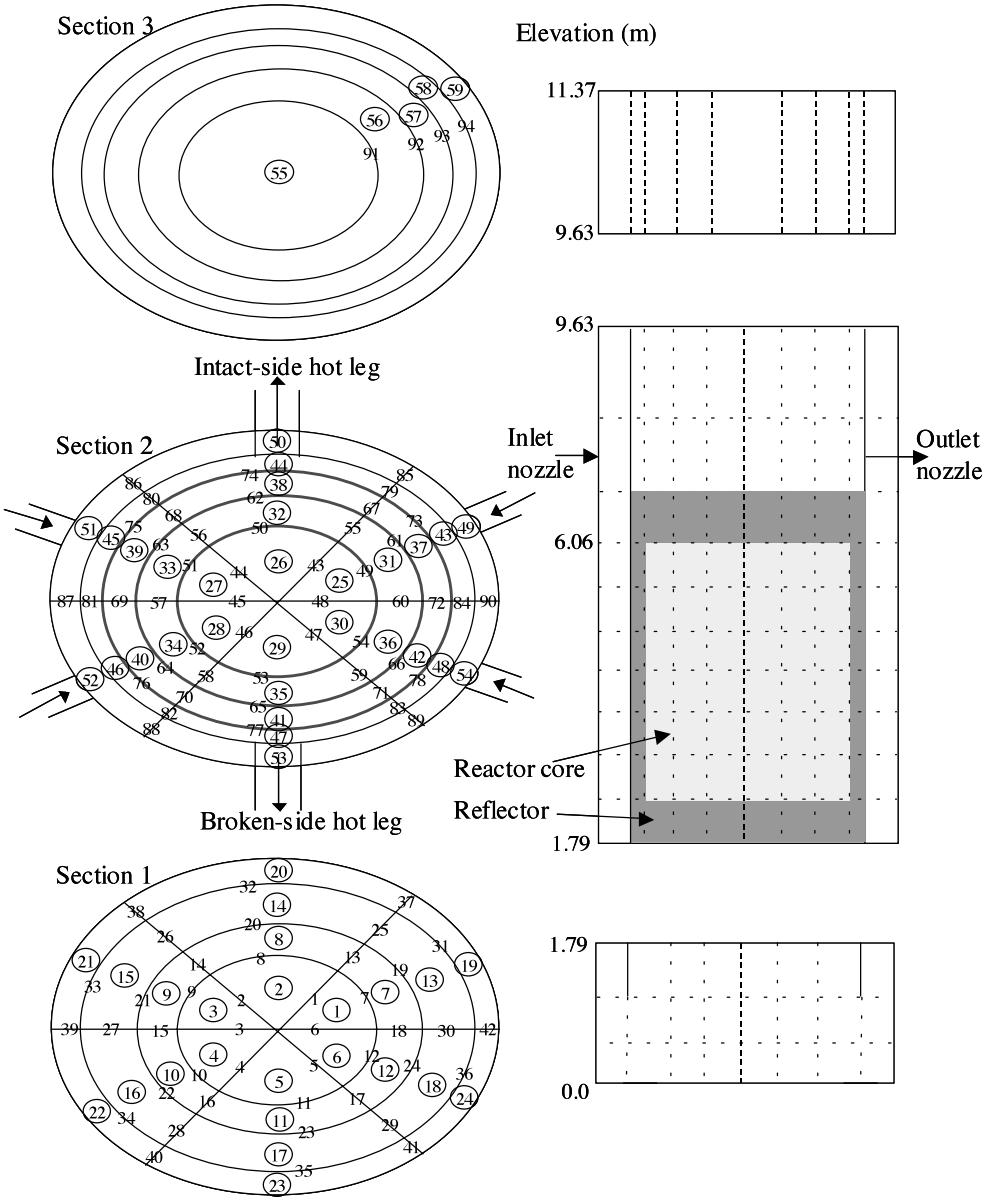

Fig. 3. Reactor vessel 3-D nodalization.

is 5 to 6% more than that entering the middle region, while the flow entering the outer region is less. The nonuniform flow distribution at the inlet, however, becomes uniform at the outlet because of the flow mixing due to cross flow. Note that a group of COBRA-III flow channels assigned to the same MARS flow channel has the same inlet flow condition since the MARS channels are large.

III.C. Transient Results and Calculation Performance

The primary transient calculation results are displayed in Figs. 4 through 9. As shown in Fig. 4, the core power starts to decrease right after the break of the steam line occurring at time 0 due to the rapid depressurization resulting in the negative reactivity insertion. The transport of overcooled water into the core then brings positive reactivity into the core to cause the core power to increase. Among the two setpoints specified in the benchmark (high neutron flux of 114% and low RCS pressure of 13.41 MPa), the low-pressure setpoint is reached first as identified in Fig. 5 showing the pressures at various locations in the system. The trip signal is thus initiated at 5.5 s, and 0.5 s later, the scram is activated so that the core power decreases rapidly from the maximum core power of 111.5%. The scram is completed in 2.2 s, and

TABLE I

Primary Steady-State Results of the Base MARS/MASTER Case

Parameter	Design	MARS/MASTER	Difference
RCS pressure (MPa)	14.96	14.98	+0.02 MPa
RCS flow rate (kg/s)	17 602	17 606	+0.02%
Core flow rate (kg/s)	16 052	15 955	−0.6%
Cold leg temperature (K)	563.8	563.9	+0.1 K
Hot leg temperature (K)	591.4	591.8	+0.4 K
Temperature rise (K)	27.6	27.9	+1.1%
SG inventory (kg)	26 000	27 006	+3.9%[a]
k_{eff}	1.00361		
$F_r/F_z/F_q$[b]	1.332/1.098/1.475		
Axial offset, %	−3.9		
Maximum centerline/average fuel temperature (K)	1499.6/906.3		

[a]This is 2.4% if the amount of water in the feed line between the feedwater isolation valve and the SG inlet nozzle is included.
[b]Radial/axial/3-D assembly-wise peaking factors, not pinwise.

TABLE II

Average Assembly Flow Rates in Each Flow Channel*

	Inner Region (7.5 FAs/Section)			Middle Ring (10 FAs/Section)			Outer Ring (12 FAs/Section)		
Sector[a]	Inlet	Outlet	Difference	Inlet	Outlet	Difference	Inlet	Outlet	Difference
1	95.9	89.9	−6.1	90.8	90.3	−0.6	85.3	90.3	5.1
2	94.6	89.8	−4.7	92.8	90.1	−2.7	86.5	90.2	3.7
3	95.9	89.9	−6.1	90.8	90.3	−0.5	85.3	90.3	5.1
4	96.0	89.8	−6.1	90.8	90.3	−0.6	85.3	90.3	5.1
5	94.6	89.8	−4.8	92.8	90.1	−2.7	86.5	90.2	3.7
6	96.0	89.8	−6.1	90.8	90.2	−0.6	85.3	90.3	5.1

*The flow rates are in kilograms per second.
[a]Sector 1 is located at the first quadrant contacting the *x* axis, and the sectors are numbered counterclockwise. Sectors 2 and 4 are connected to the two hot legs, while the other four are connected to the cold legs. The stuck rod is located in sector 6 of the outer ring.

the maximum negative reactivity of 5.85 $ occurs at 8.1 s as shown in Fig. 6. Simultaneously with the scram signal, the turbine stop valve closes so that pressure builds up in the intact SG as identified in Fig. 5.

The overcooling of the coolant continues as the excessive heat removal by the broken SG goes on. The inlet temperature thus decreases continuously as shown in Fig. 7, and the associated positive reactivity insertion brings the core back to critical at 60.6 s (Fig. 6). In the meantime, the subcritical neutron multiplication makes the core return to power. The maximum return-to-power of 36.8% occurs at 67.2 s. The decrease in the core reactivity and power beyond the peak point is caused by the dryout of the broken SG and subsequent negative thermal feedback effects. As shown in Fig. 8, the SG becomes nearly empty at ~70 s, and no more overcooling occurs after that. The coolant temperature then monotonically increases because of the heatup in the core, and the core power goes down.

During the transient calculation, MARS maintains small time step sizes that are limited by the steam flow in the broken steam line. As shown in Fig. 9, the MARS time step size is 5 to 10 ms for the time when the steam discharge continues. These time step sizes are far too small compared with the suitable time step sizes of the MASTER neutronics and COBRA-III core T-H calculations for this slow transient. Hence, in MASTER, the minimum time step size was set to 100 ms, so the number of the MASTER neutronics calculation is about 1000 for the 100-s simulation. This cumulative explicit MASTER calculation scheme results in a considerable reduction in the computing time as shown in Table III. The

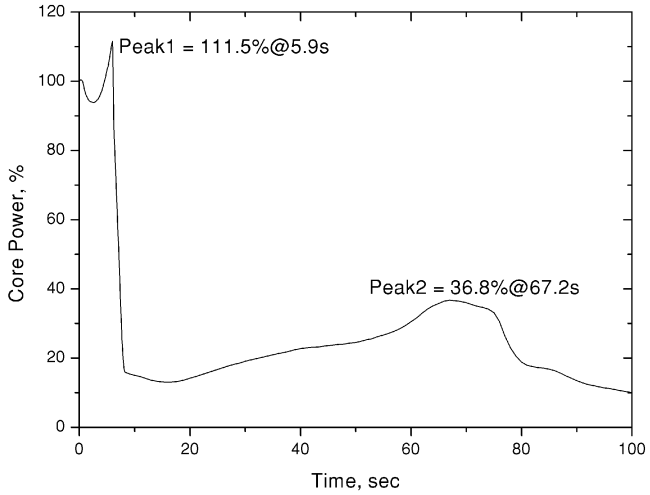

Fig. 4. Transient core power.

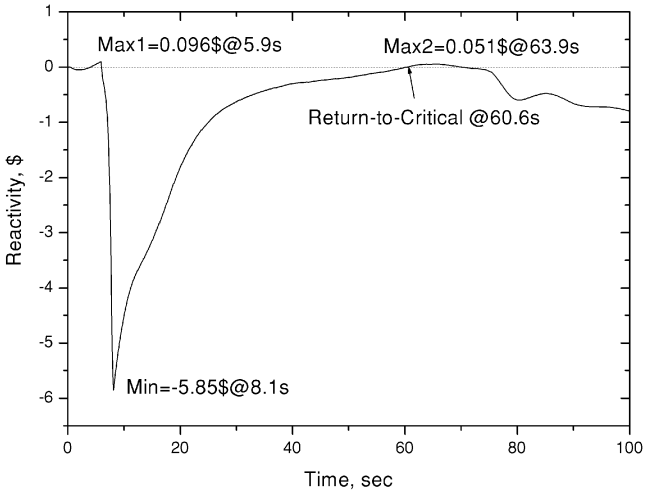

Fig. 6. Transient core reactivity.

time for the MASTER calculation (including COBRA-III T-H) is only 18% of the total computing time because the MASTER calculation is performed only once per about 13 MARS calculations on the average. This result demonstrates the effectiveness of the MARS/MASTER coupled calculation control logic described in Sec. II.C.

IV. SENSITIVITY STUDIES ON CORE T-H NODALIZATION

The refined core T-H calculation results reported previously were somewhat different from the earlier results[2] obtained by using the original MARS/MASTER coupling scheme based on the single coupling for the coarse core T-H nodalization. Besides the k_{eff} that is lowered by $\sim 210 \times 10^{-5}$, the steady-state power distribution and the transient core power behavior are noticeably different. In order to understand the difference, sensitivity studies were performed using four different core T-H nodalization schemes. The first case is the single coupling case—the old case with the coarse core T-H nodalization scheme employing 18 channels and 6 axial levels in the active core. The other three cases are all double coupling cases, but with different COBRA-III

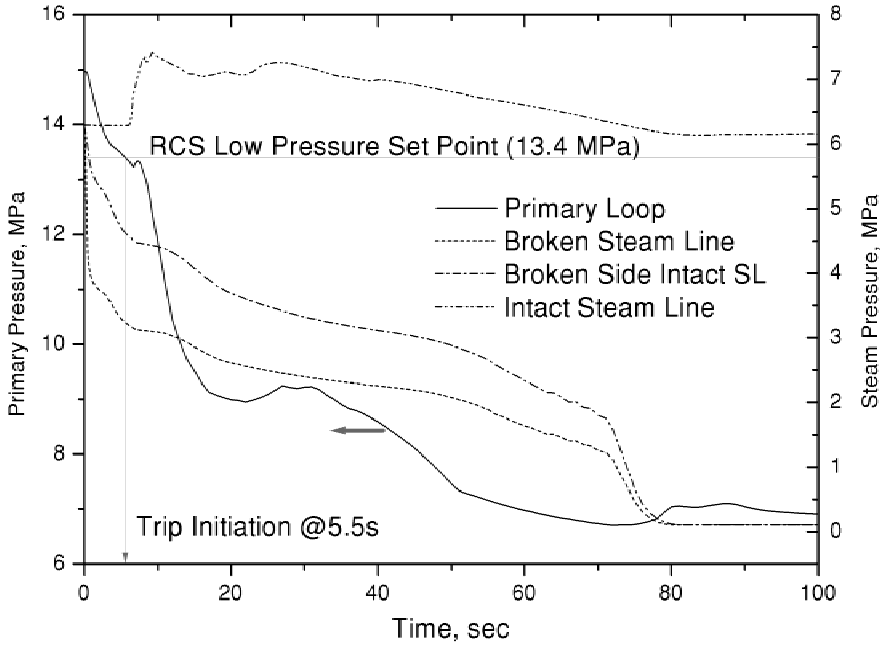

Fig. 5. Transient primary and secondary system pressure.

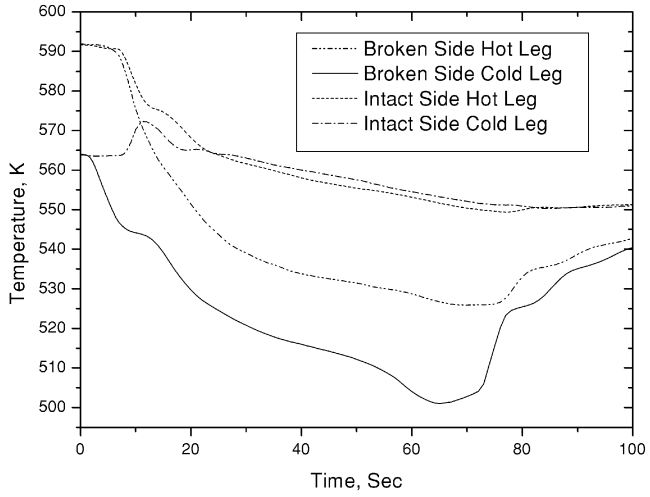

Fig. 7. Transient coolant temperatures.

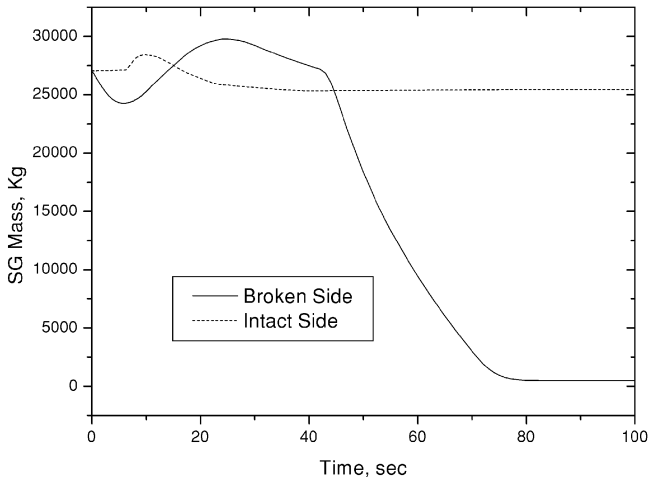

Fig. 8. Transient SG inventory.

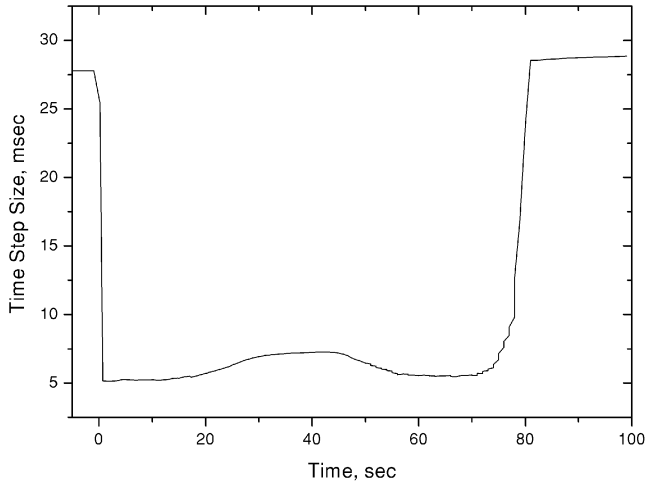

Fig. 9. MARS time step size variation during the transient.

TABLE III

Computing Time and Number of Calls of Each Module

Module	Time (s)[a]	Fraction (%)	Number of Calls
MARS T-H	2013	82.3	13 598
MASTER flux	187	7.6	1 012
COBRA-III	141	5.8	1 012
MASTER others	105	4.3	—
Total	2446	100.0	—

[a]CPU time measured on a personal computer equipped with a 1-GHz Pentium-III CPU.

nodalizations. The second case employs the same nodalization as the first case, while the third case is for the axial refinement of the second case employing 24 axial levels. The fourth case, which employs the same core T-H nodalization as the base case, is for the radial refinement of the third case employing 177 channels—one channel per assembly. In reality, however, the second and third cases also employ one channel per FA, but a group of channels is made to be identical by assigning the same power generation rate and by blocking cross flow. In other words, the COBRA-III flow channels belonging to the same coarse T-H channel are identical parallel channels with no lateral flow. In order to be consistent with this "no-cross-flow" situation, the MARS model is constructed with very large flow resistance in the gaps located in the active core region. The fourth case also employs the no-cross-flow option in the COBRA-III calculation. In Secs. IV.A and IV.B, the steady-state results of the four cases are first compared, and the transient results of the normal single coupling case (with cross flow) are compared with the base case results.

IV.A. Comparison of Steady-State Results

The key output parameters characterizing the steady-state core obtained from the four cases are compared in Table IV. First, slight differences are noted between cases 1 and 2, which employ the same core T-H nodalization. These differences originate from the fact that COBRA-III results are used for feedback calculations in case 2, while only the MARS results are used in case 1. There are several differences noted in the property data and the solution method of the MARS and the COBRA-III T-H modules. For example, the water property data and heat transfer coefficient correlations are also different. Furthermore, the T-H to neutronics mapping scheme of the COBRA-III–based MASTER calculation is different from that of the MARS-based calculation. Axially, a linear interpolation scheme is employed to estimate fine node

TABLE IV

Steady-State Output Parameters of the Four Sensitivity Study Cases

	Single Coupling 18 Channels/ 6 Planes(1)[a]	Double Coupling			Remarks for the Difference Between Cases 1 and 4
		18 Channels/ 6 Planes(2)	18 Channels/ 24 Planes(3)	177 Channels/ 24 Planes(4)	
k_{eff}	1.00569	1.00528	1.00517	1.00361	206×10^{-5} decrease
F_r	1.3321	1.3317	1.3316	1.3299	Peak at different locations
F_z	1.0724	1.0595	1.0481	1.0979	From top to bottom skewed
Average T_c (K)	579.3	579.7	579.8	580.0	0.7°C increase (43×10^{-5})[b]
Average T_f (K)	820.6	826.7	827.0	829.4	8.8°C increase (23×10^{-5})[c]
Maximum T_f (K)	899.2	902.4	915.1	961.3	62°C increase

[a]The case number is in parentheses.
[b]Based on MTC = 62×10^{-5}/K (final specification value).
[c]Based on fuel temperature coefficient = 2.6×10^{-5}/K (final specification value).

coolant temperatures, and densities from the coarse mesh results in the double coupling mode, while a constant value is assigned to all the fine nodes belonging to the coarse node in the single coupling mode. Despite these differences in the data and methods, the differences in the output parameters between cases 1 and 2 are negligible. This is identified in Fig. 10 as well, comparing the steady-state axial power distributions.

Between cases 2 and 3, only the axial nodalization is different in the model. This difference is reflected on the maximum fuel temperature, but the average properties remain essentially the same, and thus, the axial refinement turns out to be not very effective. The radial refinement, however, introduces significant changes in the characteristics' parameters. First of all, the k_{eff} is reduced by 206×10^{-5} from case 1 to 4. The core average coolant and fuel temperatures are increased by 0.7 and 8.8°C, respectively. The axial power distribution becomes bottom skewed as shown in Fig. 10. The relative assembly power is different by up to 4.4%. All of these differences are related to each other as explained below.

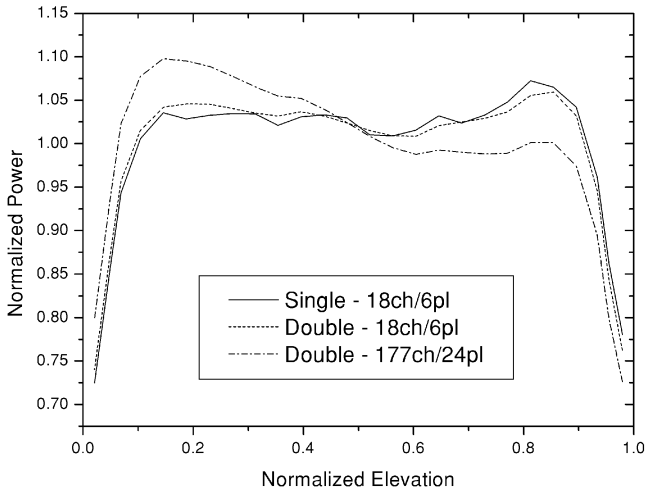

Fig. 10. Steady-state axial power comparison.

The coarse T-H calculation tends to increase the extent of nonuniformity in the power distribution because the higher-power assemblies experience less negative feedback with the coarse T-H nodalization than they do with the refined T-H nodalization. This originates from the fact that the average power of the assemblies belonging to the coarse T-H node is used to determine the thermal condition, and thus, the temperature in the high-power assembly is underestimated. As a result, the power (and also the neutron flux) at the lower-power assemblies located at the core periphery decreases. The decrease in the peripheral flux results in lower neutron leakage, and consequently, the k_{eff} of the coarse mesh case would be larger. Conversely, the reactivity would decrease with the refined calculation.

The extent of the reactivity decrease due to the reduction in radial leakage in the refined calculation would be small near the core bottom region since the coolant temperature is uniform at this region and no differences are noted between the results of coarse and fine T-H nodalizations. The difference would increase as the flow moves up. Thus, the reactivity at the planes near the top would be smaller with the refined nodalization than with the coarse nodalization. This would cause the decrease in the core power in the upper region and consequently the bottom skewed power shape as identified in Fig. 10. The increase in the axial peaking factor would cancel out somewhat the decrease in the local peaking factor attained by the refined feedback. The bottom skewed power shape causes the average coolant temperature to increase because the coolant heats up earlier. The increase in the coolant temperature brings in another reason for the decrease in core reactivity. The 0.7°C increase in the coolant average temperature would amount to a 43×10^{-5}

decrease for a moderator temperature coefficient (MTC) value of 62×10^{-5}/K.

The reduction in k_{eff} with the refined nodalization has a nontrivial impact in the transient behavior through the reduced posttrip subcriticality, which is defined as the reactivity difference between the hot-full-power (HFP) all-rods-out (ARO) state and the scrammed state. Suppose a core state after the scram. The core power will be very low, and thus, there will be little difference in reactivity between the coarse and fine node calculations for this state. Thus, the posttrip subcriticality will be smaller if the reactivity of the initial HFP ARO is smaller given the same reactivity of the scrammed state. The smaller posttrip subcriticality would cause a faster and higher rise of core power as demonstrated in Fig. 11.

IV.B. Comparison of Transient Results

The transient core power change of the refined T-H nodalization case is compared in Fig. 11 with that of the coarse T-H nodalization. Although the difference is not large, the coarse nodalization case underestimates the level of return-to-power with a slower rise around 20 s. This trend was also observed in a study on nodalization for exercise II with SAS-DIF3DK (Ref. 11). The reason behind this trend is believed to be the overprediction of the posttrip subcriticality with the coarse nodalization as discussed in Sec. IV.A.

The underprediction of the maximum return-to-power shown in Fig. 11 is merely an 0.8% point. Thus, the significance of the refined core T-H nodalization can be neglected in the aspect of the global core power level. The local power, however, reveals large errors with the coarse T-H nodalization as shown in Fig. 12, which shows the relative nodewise (not pinwise) peak linear power density. At the time of maximum return-to-power, the

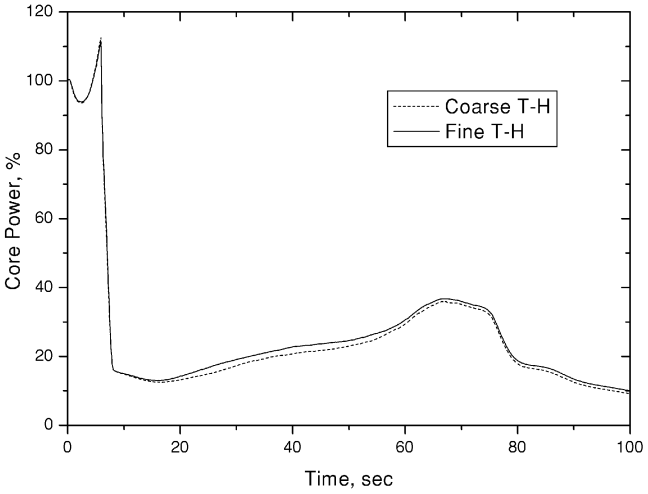

Fig. 11. Transient core power comparison.

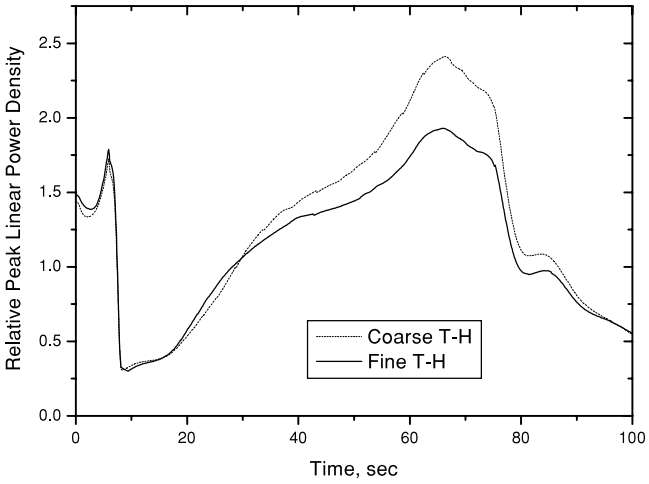

Fig. 12. Transient local peak power comparison.

coarse nodalization case overestimates the peak power by 25% (from 1.93 to 2.41). The primary contribution to this 25% local power error comes from the error in the radial power distribution as shown in Fig. 13. The radial power error is almost 16% near the stuck rod region, which has the highest power. This is because the

0.542	1.129	0.931	1.316	0.769	1.333	0.769	0.436
-5.3	-3.6	-2.4	-1.2	-2.0	-1.8	-2.6	-3.7
1.330	1.033	1.649	1.274	1.872	1.370	1.730	0.661
-2.8	-1.5	0.9	1.6	1.3	0.0	-0.2	-2.8
1.195	1.824	1.433	2.308	1.981	2.391	1.617	0.638
-0.8	2.8	4.3	6.6	5.5	4.5	2.3	-1.1
1.802	1.488	2.452	1.904	2.939	1.838	1.422	
1.6	5.2	8.8	9.0	11.0	8.3	5.9	
1.115	2.295	2.215	3.062	2.778	2.891	1.163	
1.3	7.0	10.3	13.0	15.1	14.2	9.4	
2.083	1.755	2.785	1.976	2.963	1.725		
3.2	7.4	11.7	12.2	15.8	13.8		
1.244	2.285	1.948	1.587	1.221	← Ref.		
3.9	9.6	11.6	12.4	12.2	← Error (%)		
0.713	0.891	0.792					
2.9	6.8	8.6					

* The fuel assemblies belonging to the same MARS flow channel have the same shade. The dashed box indicates the stuck rod position.

Fig. 13. Relative error in the radial power distribution at the time of maximum return-to-power for the coarse nodalization case.

temperature in the high-power assembly is significantly underpredicted with the coarse nodalization since the average of 12 temperatures including those of the very lower power assemblies is used for all 12 assemblies. Because the error in the local power is reflected directly in the DNBR calculation, it is very important to have accurate local power distributions in the safety analysis. It is shown here that the refined core T-H nodalization enhances considerably the accuracy of local power peaking.

V. DNB CALCULATIONS

The MASTER code employs a simplified DNB calculation model in which the critical heat flux (CHF) of the hot channel in each assembly is estimated from coarse-channel (a fuel assembly or its quarter-sized channel) T-H calculation results. In order to estimate conservatively the hot channel CHF, which is a function of local quality, mass flux, and pressure, from the assembly average T-H calculation results, a special hot channel model employing the pin-to-box factor and the flow penalty factor is used. Specifically, the local enthalpy determining the local quality is estimated multiplying the pin-to-box factor to the channel average enthalpy rise. The pin-to-box factor is determined for each assembly from the pin power reconstruction calculation at each time step. It is augmented by an uncertainty factor specified in the input. On the contrary, the mass flux is reduced by a certain fraction for conservatism. The local quality and the mass flux determined as such are then used to determine the CHF from a correlation chosen out of several available ones. The actual hot channel heat flux is obtained by multiplying the pin-to-box factor to the channel average heat flux. The CHF and the actual heat flux then determine the hot channel DNBR.

The simplified DNB calculation feature of MASTER was used in the coupled MARS/MASTER calculation for the OECD MSLB benchmark in order to examine the possibility of the onset of DNB in this problem. Since the primary pressure reduces to below 45% of the nominal pressure and inlet subcooling is large during the MSLB transient, a wide range CHF correlation called the 1995 lookup table[12] was chosen for this problem. The lack of form functions needed for pin power reconstruction was overcome by the use of a large uncertainty (20%) in the pin-to-box factor. The minimum DNBR (MDNBR) obtained as such is displayed in Fig. 14. In Fig. 14, the initial MDNBR is 3.08, and the lowest value during the transient is 2.57 around 70 s. Despite the strong power peaking near the stuck rod and reduced pressure, the MDNBR stays far above 2.0 throughout the transient. This is possible because inlet subcooling is very large in the broken side as identified in Fig. 15, which shows the flow quality change along the channel in which the MDNBR occurs.

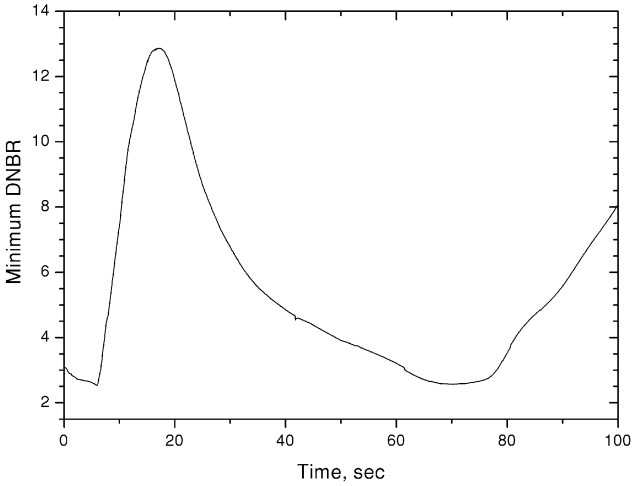

Fig. 14. Transient MDNBR change.

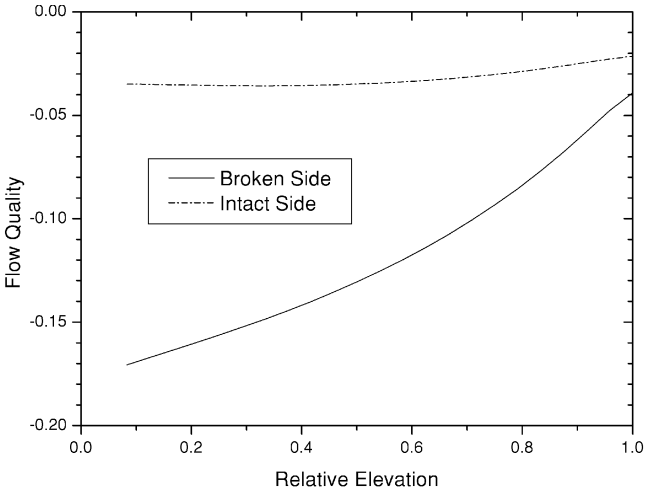

Fig. 15. Flow quality change along the flow channel at the time and channel of MDNBR.

VI. CONCLUSIONS

The solution accuracy of the MARS/MASTER coupled system T-H spatial kinetics code was enhanced significantly by the feature of refined core T-H nodalization. The feature was realized by the double coupling scheme that introduces the isolated COBRA-III core-only T-H calculation based on MARS-generated flow boundary conditions. The most important improvement attainable with a refined nodalization is the accuracy enhancement in the local power prediction. As demonstrated for the transient calculation for the MSLB problem, detailed thermal feedback reduces the peak local power by up to 25%. Since local power information is necessary for the determination of fuel melting and DNB, coupled codes

are required to have a refined core nodalization feature for accurate prediction of such safety-related phenomena. Minor impacts of T-H node refinement are observed in the core reactivity and consequently in the posttrip subcriticality. With a finer nodalization, the initial core reactivity decreases by up to 200×10^{-5}, and the core power increases slightly faster during the MSLB transient due to the reduced posttrip subcriticality. The additional computational cost for refined calculations can be made negligible by employing the double coupling scheme and also the cumulative explicit core calculation logic resulting in much larger time step sizes for core neutronic and T-H calculation. The demonstrative DNB calculation for the MSLB problem shows that DNB does not occur because of the large amount of inlet subcooling in the broken side despite the strong power peaking near the stuck rod and low pressure.

REFERENCES

1. K. IVANOV, T. BEAM, and A. BARATTA, "Pressurized Water Reactor Main Steam Line Break (MSLB) Benchmark, Volume 1: Final Specifications," NEA/NSC/ DOC(99)8, OECD/NEA, Organization for Economic Cooperation and Development/Nuclear Energy Agency (1999).

2. J.-J. JEONG et al., "MARS/MASTER Solution to OECD Main Steam Line Break Benchmark Exercise III," *J. Korean Nucl. Soc.*, **32**, 214 (2000).

3. J.-J. JEONG, K. S. HA, B. D. CHUNG, and W. J. LEE, "Development of a Multi-Dimensional Thermal-Hydraulic System Code, MARS 1.3.1," *Ann. Nucl. Energy*, **26**, 1611 (1999).

4. B. O. CHO et al., "MASTER-2.0: Multi-Purpose Analyzer for Static and Transient Effects of Reactors," KAERI/TR-1211/99, Korea Atomic Energy Research Institute (1999).

5. J. JACKSON and N. TODREAS, "COBRA III-C/MIT-2: A Digital Computer Program for Steady State and Transient Thermal Hydraulic Analysis of Rod Bundle Nuclear Fuel Elements," MIT-EL81-018, Massachusetts Institute of Technology (1981).

6. H. G. JOO et al., "Significance of Refined Core Thermal-Hydraulic Nodalization in the MSLB Analysis," *Trans. Am. Nucl. Soc.*, **84**, 29 (2001).

7. H. G. JOO, B. O. CHO, Y. J. YOO, and S. Q. ZEE, "Analysis of OECD MSLB Benchmark Exercise II Using the MASTER Code," *Proc. Int. Conf. Mathematics and Computation, Reactor Physics and Environmental Analysis in Nuclear Applications*, Madrid, Spain, September 27–30, 1999, p. 343 (1999).

8. REALP5 CODE DEVELOPMENT TEAM, "RELAP5/MOD3 Code Manual," NUREG/CR-5535, Idaho National Engineering Laboratory, U.S. Nuclear Regulatory Commission (1995).

9. M. J. THURGOOD et al., "COBRA/TRAC—A Thermal-Hydraulic Code for Transient Analysis of Nuclear Reactor Vessels and Primary Coolant Systems," NUREG/CR-3046, U.S. Nuclear Regulatory Commission (1983).

10. R. BOER, H. FINNEMANN, and A. KNOLL, "MSLB Exercise 2: 3-D Kinetics Results with RELAP5/PANBOX," *Proc. Int. Topl. Mtg. Advances in Reactor Physics and Mathematics and Computation into the Next Millennium (PHYSOR 2000)*, Pittsburgh, Pennsylvania, May 7–12, 2000, American Nuclear Society (2000) (CD-ROM).

11. T. TAIWO, F. E. DUNN, J. E. CALAHAN, and H. S. KHALIL, "OECD/NEA PWR MSLB Sensitivity Studies Using SAS-DIF3DK," *Proc. Int. Conf. Mathematics and Computation, Reactor Physics and Environmental Analysis in Nuclear Applications*, Madrid, Spain, September 27–30, 1999, p. 333 (1999).

12. D. C. GRONEVELD et al., "The 1995 Lookup Table for Critical Heat Flux in Tubes," *Nucl. Eng. Des.*, **163**, 1 (1996).

Han Gyu Joo (BS, 1984, and MS, 1986, nuclear engineering, Seoul National University, Korea; PhD, 1996, nuclear engineering, Purdue University) is employed by Korea Atomic Energy Research Institute (KAERI). He used to work on nodal kinetics codes such as PARCS, ARROTTA, and MASTER. His interest these days is to develop a three-dimensional whole core transport code DeCART as the neutron kinetics module of the *Numerical Nuclear Reactor*.

Jae-Jun Jeong (BS, nuclear, engineering, Seoul National University, Korea, 1984; PhD, nuclear engineering, Korea Advanced Institute of Science and Technology, 1990) is employed by KAERI. His current interests include nuclear reactor thermal hydraulics (T-H), best-estimate system code development, and advanced reactor system design.

Byung-Oh Cho (BS, nuclear engineering, Seoul National University, Korea, 1983; PhD, nuclear engineering, Oregon State University, 1990) is a principal

researcher at KAERI. His current interests include reactor physics and core design and analysis code development.

Won Jae Lee (BS, 1978; MS, 1984; and PhD, 1993, nuclear engineering, Seoul National University, Korea) is a principal researcher at KAERI. He was a project manager of the MARS T-H system code development. His current interests include the T-H safety of nuclear reactors and the development of advanced nuclear reactors.

Sung-Quun (Sung-Kyun) Zee (BS, materials science and engineering, Seoul National University, Korea, 1975; MS, nuclear engineering, Ohio State University, 1979; PhD, nuclear engineering, North Carolina State University, 1987) is employed by KAERI. He is currently the manager of the Core Design and Analyses Technology Department developing the SMART advanced integral reactor core design and analysis methods including nodal diffusion methods, neutron transport methods, spatial kinetics methods, core T-H methods, core monitoring and protection methods and numeric algorithms for parallel computers. His background includes pressurized water reactor core design and operations, and transient analysis.